weighting is performed by creating a (Weiner) temporal filter matched to the correlation properties of the atmosphere on a particular occasion. In this way one can achieve the highest possible number of reference photons (avoiding purely statistical fluctuation in centroid position) without integrating into the image genuine atmospheric movement. In the case of a bright reference the effective integration time can be reduced. The star profiles of the sharpened image have rather sharp cores indicating that a further stage of improvement can be expected from image selection – we would also expect that there will be a further improvement when the centroid is determined by reference to the brightest region in the composite reference, a method which we have previously demonstrated with MAMA data (of M15, using the 4.2-m WHT). In a number of cases groups have stars that have become resolved in the sharpened image compared to the raw image – which would have been considered to be of good resolution until recently.

Figure 3: TRIFFID has the ability to perform image sharpening in two colours simultaneously. The MAMA is used on a straight-through optical path to perform blue imaging and to give information about image motion and width. The same information is applied to the side-arm detector, which is in this case the RAL-PCD, imaging in the red. The RAL-PCD is an image intensifier plus CCD real-time centroiding photon-counting camera. A narrow strip of the photocathode (50 by 500 pixels) is read out every 7 milliseconds, which produces 200 by 2,000 pixels after centroiding in an array of Transputers. The image scale is 1.7 times larger than the MAMA. The image is the result of derotation and sharpening using the MAMA centroid – the resultant resolution is 0\".7, comparable with that of the MAMA. The field looks quite different from the blue image.

Figure 4: The side-arm image sharpening does not have the same requirement for large numbers of reference photons which plagues most high-resolution imaging techniques – since the sharpening information is transferred from the straight-through arm. In fact, the Hα image displays the best final resolution at 0\".5 – the maximum gain allowed in theory. One purpose of narrow band imaging in the crowded centre fields of globular clusters, for example, is to look for activity which might be indicative of the presence of a cataclysmic variable star.

These images were achieved in conditions of only moderate seeing. In better seeing we have demonstrated that the process improves faster than the relative improvement in seeing. In better seeing the pupil sizes can be increased (this sort of image sharpening optimally uses pupils which are 3.5–4 times the diameter of the diffraction-limited telescope which would reproduce the seeing-limited image width), thereby increasing count rates, thereby changing the optimization between Weiner filter width and atmospheric correlation time.

This work has been partly supported by EOLAS – The Irish Science & Technology Agency – and by the University College Galway Development Fund.

Wolf-Rayet Stars Beyond 1 Mpc: Why We Want to Find Them and How to Do It

G. TESTOR, Observatoire de Paris, Section de Meudon, DAEC, France
H. SCHILD, Dept. of Physics and Astronomy, University College London, UK

1. Why

Wolf-Rayet stars are luminous objects with broad and conspicuous emission lines. In principle they can be observed out to large distances. Over many years of intensive search and with contributions from many workers, a practically complete catalogue of the WR population in the Magellanic Clouds has been obtained. In other local group galaxies similar searches were conducted and individual WR stars have been identified in most of them.

Here we report about our efforts to extend this search beyond the local group into the Sculptor group of galaxies. We selected NGC 300 as a suitable member of this group because its inclination to the line of sight is relatively small. Its distance modulus of 26 mag corresponds to 1.5 Mpc thus giving a scale of 7 pc per arcsec and allowing under good seeing conditions to resolve areas of about 6 pc. In spite of the low spatial resolution we expect that most of the WR stars can be observed individually, i.e. uncontaminated by other WR stars. If we take the spatial distribution of WR stars in the LMC as a guideline, we see that about half of them are located in large OB associations (15 pc to 150 pc) (Breysacher, 1988) and almost all of the others are widely scattered in the galaxy (Pitault, 1983). Only a few per cent are found in dense structures like the tight clusters ($\leq$ 5 pc) in the 30 Doradus area (Moffat 1987, Schild and Testor 1992). Such 30 Dor-like concentrations of massive stars are extremely bright and can be observed to distances even far beyond the Sculptor group. Broad WR emission features have indeed been found in many giant H II regions and H II galaxies (see eg. Arnault et al. and references therein). From these objects we can however only obtain synthetic information about the population of the massive stars as a whole. If possible, it is preferable to trace WR stars individually and consequently to study them in various environments because:

- The frequency and subtype distribution of WR stars in a galaxy provides fundamental clues in relation to stellar evolution theory. Metallicity effects are currently thought to dominate most aspects of a WR population (see e.g. Azzopardi et al. 1988, Arnault et al. 1989). The size of the convective core of a massive star together with mass loss processes which remove the outer hydrogen rich layers determine the predicted number of WR stars and the WN/WC ratio at various metallicities (Maeder 1991).
- Deep spectroscopic observations of WR stars in M33 have established the existence of unusually narrow-lined early WC stars, a type of WR star which was not previously known to exist. The relation between subtype and line width found for galactic WC stars does not hold for these stars. The breakdown of this relationship is unlikely to be a pure metallicity effect and remains unexplained.
- WR stars are highly evolved objects

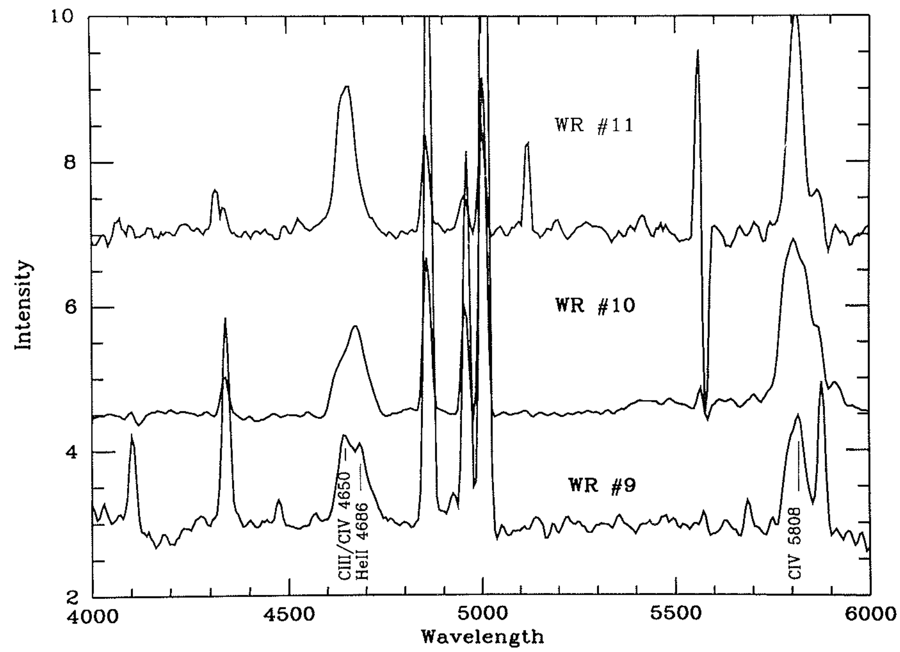

Figure 1: *Normalized spectra of WR stars number 9, 10 and 11.*

and are rapidly approaching the end of their stellar lifetime. Whether they explode as a (faint?) supernova or collapse into a black hole is unknown. Theory is unlikely to provide unambiguous answers. It is therefore important to increase the number of known WR stars to a maximum in order to increase the chances for such an event to be observable. It is incidentally an intriguing thought that the light travel time from NGC300 is much longer than the remaining lifetime of the WR stars in this galaxy and therefore these stars no longer exist today.

2. How

We decided to look into the possibilities of exploring the WR population in NGC300 with present-day ESO instrumentation. EFOSC with its high efficiency and versatility was the obvious choice. Two narrow-band filters, one centred on the strong WR emission lines between λ4650 and λ4690 Å and the other in the adjacent continuum were mounted in the filter wheel. Promising candidates could immediately be confirmed (or otherwise) by switching into spectroscopic mode. We obtained the first trial images during the night of 31 December 1989. Most surprisingly, it was possible to recognize three WR candidates already visually by just comparing the two images. Spectroscopic observations immediately confirmed the WR nature of these stars (Schild and Testor 1991). Subsequent analysis of the images with DAOPHOT revealed more candidate WR stars. We were allocated 3 nights in October/November 1991 to continue the search but the observations were hampered by bad weather and bad seeing conditions. Nevertheless we were able to obtain spectra for a handful of our candidates and confirm them as WR stars (Schild and Testor 1992).

Now we report further recent progress: Three new WR candidate stars were found and one of them was confirmed spectroscopically. We also give spectral types for the remaining WR stars No. 9 and 10 without spectra in Schild and Testor (1992). These slit spectra were obtained during the night of 31 December 1992 with the ESO 3.6-m telescope and EFOSC. We used the B300 grating giving a wavelength coverage from 3700 to 7000 Å and a resolution of 15 Å with a slit of 2″. The observations were recorded with a 520 × 570 pixel Tektronix CCD (ESO # 26). The pixel size of 27 μm projects to 0.61″ on the sky. The seeing was good (FWHM = 1″).

The spectra of the WR stars No. 9, 10 and 11 are shown in Figure 1. Star 9 is the brightest source (stellar or tight cluster) in a giant stellar association of about 100 pc diameter. We previously found a WR excess of 0.6 magnitude in the narrow-band filter images for this star. This is consistent with the spectrum which seems to be of composite WN + WC type. Figure 3 shows the spectrum of WR 9 (top) in the range λ5600 to λ6800 Å. The broad CIV λ5808 emission line is clearly visible. A supernova remnant located 8 arcsec east of star 9 was observed serendipitously (Fig. 3, bottom). The slit passed over the edge of the remnant but the high velocity dispersion in the Hα line (600 km/sec) still is well recognizable. The supernova remnant coincides with the HII region No. 79 of Deharveng et al. (1988).

WR 10 is also located in a giant cluster. It has a large WR excess (Schild and Testor 1992) and accordingly, the spectrum shows strong CIV λ4650/HeII λ4686 and CIV λ5808 emission lines. We classify the object as WC4. Two arcmin south-east of No. 10, we found a further star with a strong WR excess: WR 11. It is located in the HII region numbered 90 by Deharveng et al. (1988). The spectrum shows strong CIV λ4650 and CIV λ5808 emission and we classify it as WC4–5. Two further stars with a large excess and very likely WR stars are: No. 12 in the HII region 118 (Deharveng et al. 1988) and No. 13 lying just north of WR star 5. These stars are at present only WR candidates and require spectral confirmation.

Table 1: *List of presently known WR stars in NGC 300. Most WR stars are located in HII emission regions and the corresponding numbers of Deharveng et al. (1988) and the integrated Hα fluxes (in 10^{-16} erg s^{-1} cm^{-2}) are listed. The deprojected distance from the galactic centre ϱ* is given in arcmin.

WR	Type	HII region	Hα intensity	ϱ
WR1	WC4–6	76b	1162	0.87
WR2	WNE	98	290	1.09
WR3	WC4–5			
WR4$^{\alpha}$	WN3–6	137a	8214	3.91
WR5$^{\alpha}$	WC4–5	137b	5393	3.90
WR6	WC4–6	—		2.54
WR7$^{\alpha}$	WN7	119b	2074	3.33
WR8	WNE			5.47
WR9$^{\alpha}$	WC+WN	77	4397	3.45
WR10$^{\alpha}$	WC4	53b	3300	3.86
WR11$^{\alpha}$	WC5	90	1200	3.57
WR12		118a	4978	2.82
WR13$^{\alpha}$		137b	8214	3.91

$^{\alpha}$ indicates that the Wolf-Rayet star is a member of a giant stellar association.

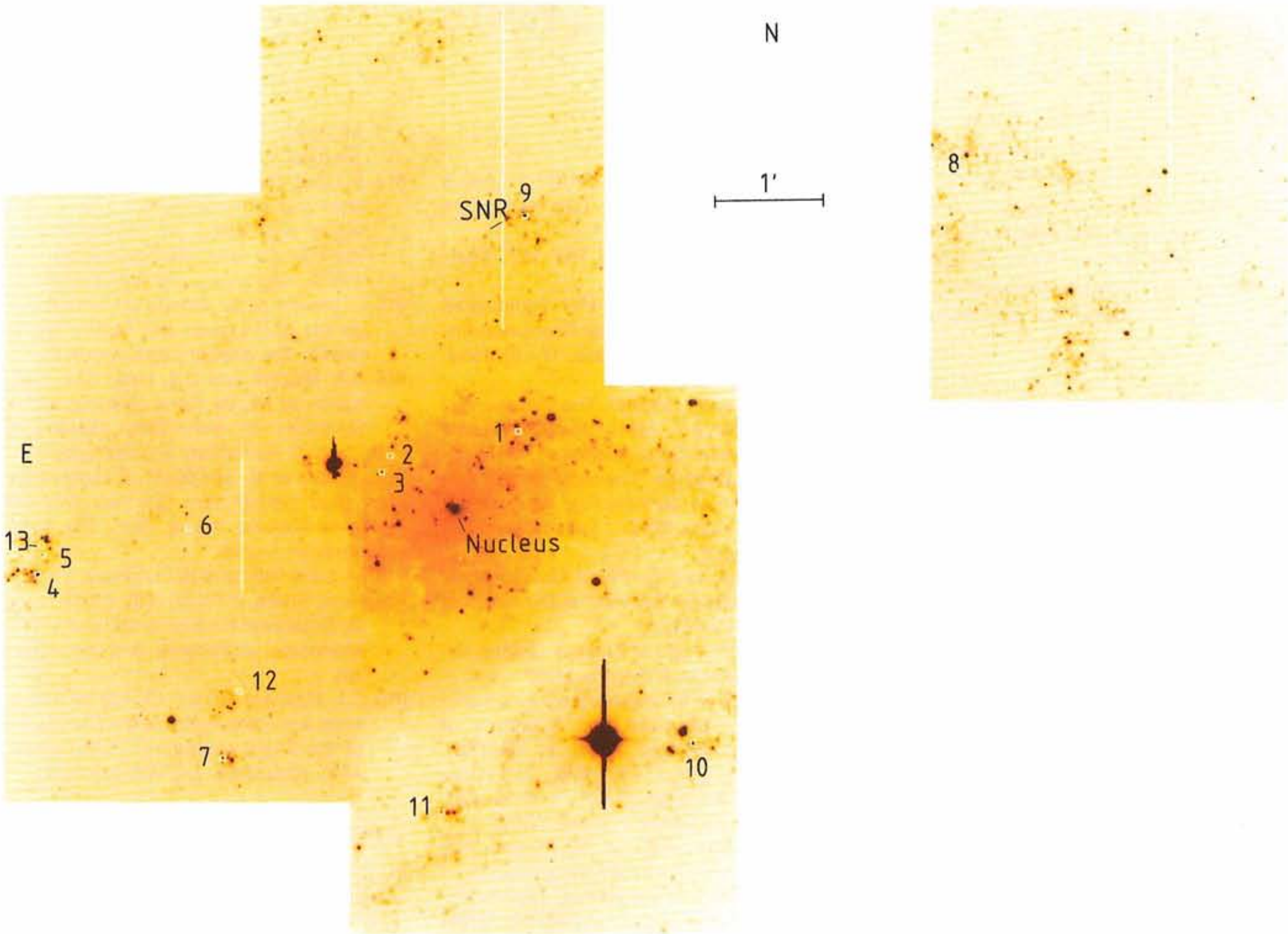

Figure 2: *Mosaic view of the parts of NGC300 which have been surveyed. The images were taken through an interference filter in the light of the WR emission feature between λ4650 to λ4690 Å. The position of the 13 WR stars listed in Table 1 are marked. The location of the serendipitously discovered supernova remnant near WR 9 is also shown. The images of the two brightest stars are heavily saturated and show vertical stripes.*

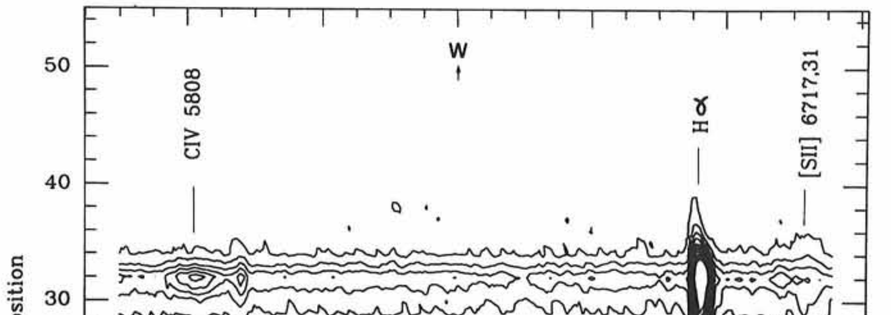

Figure 3: *Spectrum of WR 9 (top westwards) and a supernova remnant (bottom eastwards) in the range λ5600 to λ6800 Å. Note the CIV λ5808 emission feature in the spectrum of the WR star and the velocity dispersion of about 600 km/sec, the strong [NII] λ6584 and [SII] λ6717,31 emission lines in the SNR spectrum.*

In Figure 2 we present a view of the parts of NGC300 which we have imaged so far. The positions of the 11 confirmed WR stars and the 2 candidates are marked. We note that a majority of WR stars were found at galactocentric distances betweeen 3 and 4 arcmin (Table 1). This indicates that, like in other galaxies, recent formation of massive stars predominantly occurred in a ring-like structure. In Table 1 we list spectral types and data about the stellar and nebular environment of these WR stars. The spectra of many of them are of early WC type but this may be an observational selection effect because this type of WR star has particularly strong emission lines at λ4650.

Future observations will undoubtedly turn up more WR stars in NGC300. We plan to continue our search and will in a first step observe spectroscopically more of our candidate WR stars. So far all of our candidates have turned out to be WR stars because we selected first those with a large WR excess. We expect that we will however soon reach the threshold where the excesses are not very significant anymore. The continuum magnitudes of the WR stars are typically 20–21 mags and there are probably many more which are fainter. Although present day instrumentation clearly allows individual WR stars to be observed at distances beyond 1 Mpc, we find that we use it close to its limitations. In the longer term it will be necessary to use larger telescopes such as the VLT in order to complete the survey.

References

Arnault P., Kunth D., Schild H., 1989, *A&A* **224**, 73.

Azzopardi M., Lequeux J., Maeder A., 1988, *A&A* **189**, 34.

Breysacher J., 1988, Thesis, Univ. Paris VII.

Deharveng L., Caplan J., Lequeux J., Azzopardi M., Breysacher J., Tarenghi M., Westerlund B., 1988, *A&AS* **73**, 407, 423.

D'Odorico S., Rosa M., Wampler E.J., 1983, *A&AS* **53**, 97.

Maeder A., 1991, *A&A* **242**, 93.

Massey P., 1985, *PASP* **97**, 5, 24.

Pitault A., "Proceedings of a workshop held at Observatoire de Meudon" edited by M.C. Lortet and A. Pitault, 1983.

Moffat A.F.J., Niemela V.S., Philips M.M., Chu Y.H., Seggewiss W., 1987, *ApJ, 312*, 612.

Schild H., Testor G., 1991, *A&A* **243**, 115.

Schild H., Testor, G. 1992, *A&AS* **92**, 729, 748.

Schild H., Testor, G. 1992, *A&A* **266**, 145.

NEW ESO PREPRINTS

(March–May 1993)

Scientific Preprints

909. T.R. Bedding et al.: MAPPIT: Optical Interferometry with Non-Redundant Masks.
T.R. Bedding et al.: The VLT Interferometer.
Papers presented at IAU Symposium 158, "Very High Angular Resolution Imaging", Sydney, Australia, 11–15 January 1993.
910. G. Setti and L. Woltjer: The Gamma-Ray Background. *Astrophysical Journal Supplement.* Special issue of the Integral Workshop on "The Multi-Wavelength Approach to Gamma-Ray Astronomy", 2–5 February, 1993, Les Diablerets, Switzerland.
911. G. Meylan and C. Pryor: Observational Constraints on the Internal Dynamics of Globular Clusters.
P. Dubath et al.: Is There a Central Velocity Dispersion Cusp in M15?
To appear in the proceedings of a workshop in "Structure and Dynamics of Globular Clusters", held in Berkeley, California, July 15–17, 1992, to honour the 65th birthday of Ivan R. King. ASP Conference Series, in press (1993).
912. A. Sandage and G.A. Tammann: The Hubble Diagram in V for Supernovae of Type Ia and the Value of H_0 Therefrom.
913. P. Padovani and F. Matteuccl: Stellar Mass Loss in Ellipticals and the Fuelling of Active Galactic Nuclei. *The Astrophysical Journal.*
914. E. Oliva: The O I-Lyβ Fluorescence Revisited and its Implications on the Clumping of Hydrogen, O/H Mixing and the Pre-SN Oxygen Abundance in SN 1987A. *Astronomy and Astrophysics.*
915. L. Binette et al.: Effects of Internal Dust on the NLR Lyman and Balmer Decrements. *The Astrophysical Journal.*
916. P.A. Mazzali and L.B. Lucy: The Application of Monte Carlo Methods to the Synthesis of Early-Time Supernovae Spectra. *Astronomy and Astrophysics.*
917. J. Martí et al.: HH 80-81: A Highly Collimated Herbig-Haro Complex Powered by a Massive Young Star. *The Astrophysical Journal.*
918. M. Della Valle and H. Duerbeck: Study of Nova Shells. I: V1229 AQL (1970) Nebular Expansion Parallax and Luminosity at Maximum. *Astronomy and Astrophysics.*
919. I.J. Danziger et al.: Optical Spectroscopy and Photometry of the Companion of the Bright Millisecond Pulsar J0437-4715. *Astronomy and Astrophysics.*

Technical Preprint

51. B. Lopez and M. Sarazin: The ESO Atmospheric Temporal Coherence Monitor Dedicated to High Angular Resolution Imaging. *Astronomy and Astrophysics.*

Mapping the Large-Scale Structure with the ESO Multi-Slit Spectrographs

V. DE LAPPARENT, C. BELLANGER, S. ARNOUTS, Institut d'Astrophysique de Paris, France
G. MATHEZ, and Y. MELLIER, Observatoire Midi-Pyrénées et de Toulouse, France
A. MAZURE, Université des Sciences et Techniques du Languedoc, France

Preliminary Remarks

During the past decade, our understanding of the large-scale galaxy distribution has evolved drastically through the steady acquisition of redshifts of galaxies. The major optical redshift surveys of the nearby distribution ($B \leq 14.5-15.5$) are being performed using partly-dedicated telescopes of small diameter (1.5 m) or significant fractions of observing time in general facilities (see for example references [1], [2]. In these surveys, the projected density of objects is of the order of one per square degree, requiring the acquisition of the spectra one by one.

Mapping the galaxy distribution out to larger distances – and thus to fainter limiting magnitudes – requires the use of intermediate and large-size telescopes. The decrease in flux is largely compensated by the increasing projected density of galaxies, yielding a high rate of data acquisition in terms of number of redshifts per night. Multi-fiber spectrographs on 2.5 to 3.5-m telescopes allow to obtain simultaneously spectra of tens of galaxies in fields of the order of the square degree out to limiting magnitudes in the range $B = 18-20$. In these configurations, more than 100 spectra can be obtained per observing night [3], [4].

Whereas optical fibers offer a convenient way to cover fields of the order of one square degree, multi-slit spectrographs guarantee both efficiency in transmission and quality of the sky-subtraction for spectra of galaxies with limiting magnitudes $B = 22$ or fainter. The ever increasing projected density of objects allows to still benefit from the multiplex gain over the small area of a typical CCD. However, the loss in flux implies longer exposure times, and acquisition of a significant sample of objects at these magnitudes requires a large amount of observing nights on a 4-m-class telescope.

The quest for samples of galaxies which continuously increase in number of objects and/or effective distance originates from the charateristics of the galaxy distribution. Until recently, each